

Type I planet migration in a magnetized protoplanetary disk

Alissa Bans, Ana Uribe and Arie König

Department of Astronomy and Astrophysics, University of Chicago, Chicago IL, USA.

abans@uchicago.edu, auribe@oddjob.uchicago.edu



Introduction

We study the effects of a large-scale, ordered magnetic field in protoplanetary disks on Type I planet migration using a combination of numerical simulations in 2D and 3D and a linear perturbation analysis. Steady-state models of such disks require the inclusion of magnetic diffusivity. To make progress using ideal MHD, we focus on simplified field configurations, involving purely vertical (B_z) and azimuthal (B_ϕ) field components and a combination of the two. Additionally, we study the case of a wind-driving disk, in which a magnetic torque $\sim B_z dB_\phi/dz$ (where B_z and B_ϕ are the equilibrium vertical and azimuthal field components) induces vertical angular momentum transport. For each of the models we calculate the locations of the relevant resonances and of the turning points, which delineate the propagation regions of the MHD waves that transport angular momentum from the planet to the disk. We use both numerical and semianalytic methods to evaluate the cumulative back torque acting on the planet. We conclude that, under realistic (3D) circumstances, a large-scale magnetic field can slow down the inward migration that characterizes the underlying unmagnetized disk — by up to a factor of ~ 2 when the magnetic pressure approaches the thermal pressure — but it cannot reverse it. A previous inference that a pure- B_ϕ field whose amplitude decreases fast enough with radius leads to outward migration applies only in 2D. For a wind-driving disk configuration, we find the presence of a subdominant B_ϕ component whose amplitude increases from zero at $z = 0$ has little effect on the torque when acting alone, but in conjunction with a B_z component it gives rise to a strong torque that speeds up the inward migration of the planet.

Linear Perturbation Analysis

Basic Equations and Disk Response

Dynamics of disk are governed by momentum, conservation of mass, and induction equations under ideal MHD:

$$\rho \left[\frac{\partial \mathbf{v}}{\partial t} + (\mathbf{v} \cdot \nabla) \mathbf{v} \right] = -\nabla P + \mathbf{F} - \rho \nabla \psi,$$

and

$$\frac{\partial \rho}{\partial t} + \nabla \cdot (\rho \mathbf{v}) = 0,$$

$$\frac{\partial \mathbf{B}}{\partial t} + \nabla \times (\mathbf{v} \times \mathbf{B}) = 0,$$

where ρ is the mass density, ψ the gravitation potential, \mathbf{v} the velocity field, \mathbf{B} the magnetic field, and \mathbf{F} the Lorentz force density.

We calculate the disk response to the planet (perturbing potential ψ') by perturbing the equations in all 3 directions and time in Fourier space (with Fourier labels m and k_z for the azimuthal and vertical directions) and then linearizing. Details in Bans, König & Uribe (2014).

Linearized equations yield a differential equation for the radial Lagrangian displacement that can be solved at each azimuthal mode m by using *high-order adaptive step Runge-Kutta methods with 16-bit precision*:

$$A_2(r) \frac{\partial^2 \xi_r}{\partial r^2} + A_1(r) \frac{\partial \xi_r}{\partial r} + A_0(r) \xi_r = S_1(r) \frac{\partial \psi'}{\partial r} + S_0(r) \psi'$$

Initial Field Configurations

Field 1: Azimuthal and vertical Fields ($B_\phi \neq 0$ at the midplane) - Uribe, Bans, & König 2014.

Field 2: Toy Wind Model: Vertical Fields plus a growing azimuthal component ($B_\phi = 0, dB_\phi/dz \neq 0$ at the midplane). - Bans, König, & Uribe 2014. (quantities for field 2 were vertically averaged over the disk scale height, h)

Resonances

Pure **Resonances:** where the density perturbation is divergent (i.e. $A_2 = 0$)
Two main types: **Magnetic resonances** where the corotating perturbation frequency ($\sigma = m(\Omega - \Omega_p)$) is that of a slow MHD Wave, and **Alfvén resonances** where the corotating perturbation frequency is equal to that of a shear Alfvén wave traveling in the vertical direction.

$$m^2 \sigma^2 = \frac{c^2 (v_{A_z} k_z + v_{A_\phi} k_\phi)^2}{v_{A_z}^2 + v_{A_\phi}^2 + c^2}$$

Magnetic Resonance (MR) for Field 1

$$r^2 \sigma^2 = \frac{v_{A_\phi}^2 (c^2 + v_{A_z}^2)}{v_{A_\phi}^2 + v_{A_z}^2 + c^2}$$

MR in strict 2D limit ($v_z = 0$) for Field 1 enforcing strict 2D allows for a closer comparison with 2D numerical work.

$$m^2 \sigma^2 = \frac{v_{A_z}^2 v_{A_\phi}^2 + v_{A_z}^2 (v_{A_\phi}^2 k_z^2 + v_{A_z}^2 k_\phi^2) + v_{A_\phi}^2 (v_{A_z}^2 k_z^2 + v_{A_\phi}^2 k_\phi^2)}{c^2 + v_{A_z}^2 + v_{A_\phi}^2}$$

Magnetic Resonance (MR) for Field 2

$$m^2 \sigma^2 = k_z^2 v_{A_z}^2 - \partial v_{A_\phi}^2 \left(1 - \frac{h^2 m^2}{3r^2} \right)$$

Alfvén Resonance (AR) for Field 2

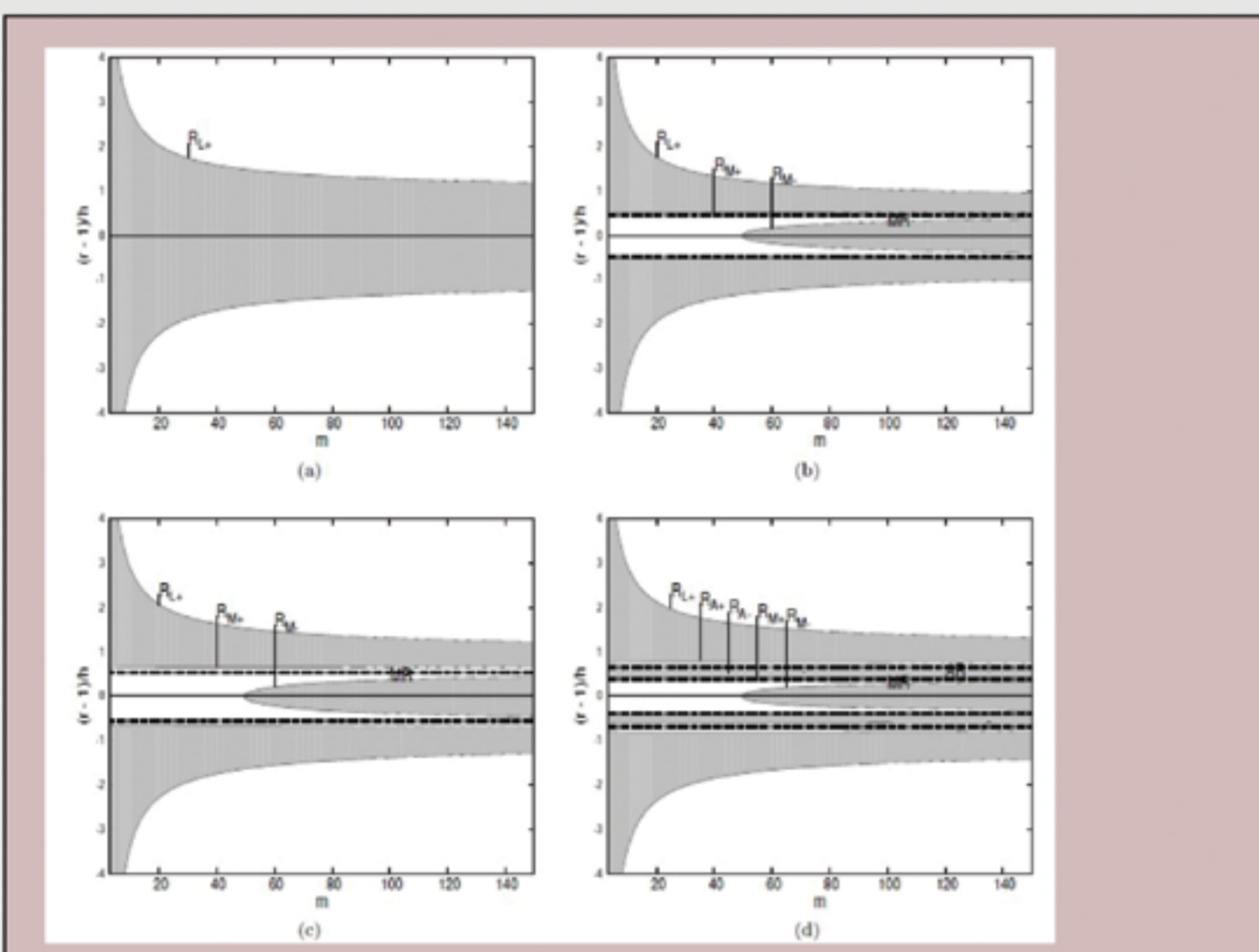
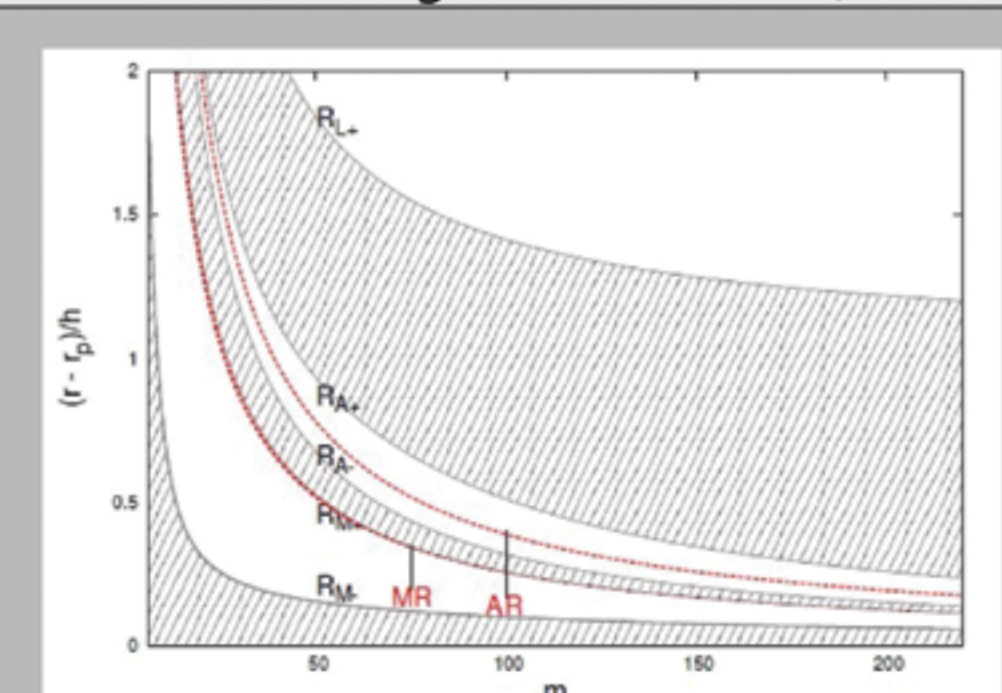
Turning Points

Where the differential equation above goes from wave-like solutions to evanescence are the so-called turning points (details for solving for the turning points are presented in Bans, König & Uribe 2014).

Vertical Fields and Toy Wind Model (2D and 3D)

Top: Wave propagation (clear) and evanescence (shaded) regions outside the planet's orbit for a purely vertical field configuration as a function of the azimuthal mode number m . The vertical wavenumber k_z and field strength are fixed. RL+, RA+, RA-, RM+, and RM- are the turning points which surround the relevant resonances (MR and AR).

Bottom: 2D (top half) and 3D (bottom half) regions of wave propagation (clear) and evanescence (shaded) for our toy wind model, shown at fixed field strengths, fixed m , and in the 3D case, fixed k_z . In 2D is a window of wave propagation immediately surrounding the planet which doesn't exist for pure vertical fields. The MR and AR locations are shown as dashed lines.



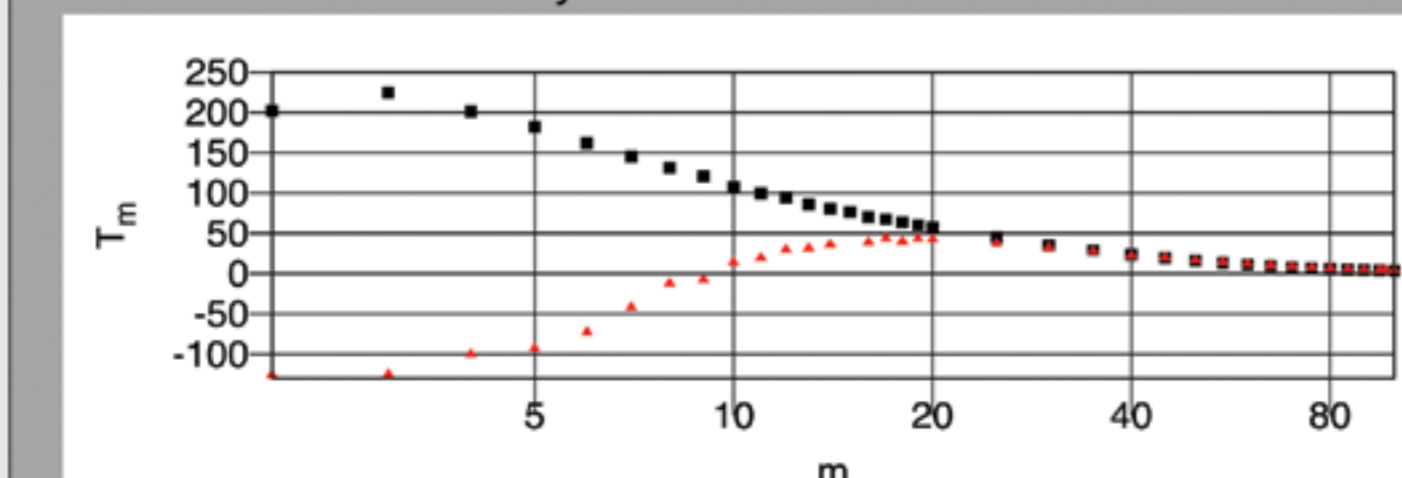
Azimuthal and Vertical Fields (2D):

Turning point locations as a function of the azimuthal wavenumber m in 2D for disks with a) vertical fields b) azimuthal fields, c) combined azimuthal and vertical fields in strict 2D (no v_z), and d) combined fields (allowing v_z). Shaded regions indicate evanescence, clear regions show wave propagation, labels starting with R show the turning locations, and the relevant resonance locations are labeled with AR or MR.

Numerical Integration Results and Total Torque

Toy Wind Model (2D):

Torque exerted by the planet on a thin uniform disk threaded by our toy wind model (black squares) in the 2D ($k_z = 0$) limit versus azimuthal wave number m . Overplotted is the case of a disk with no B field (red triangles). The cumulative torque is ~ 4000 for our toy model and ~ 1200 for the $B=0$ case, indicating that planet migration is still inwards but 3-4 times faster under the toy wind model.



Main Points Bans, König & Uribe 2014:

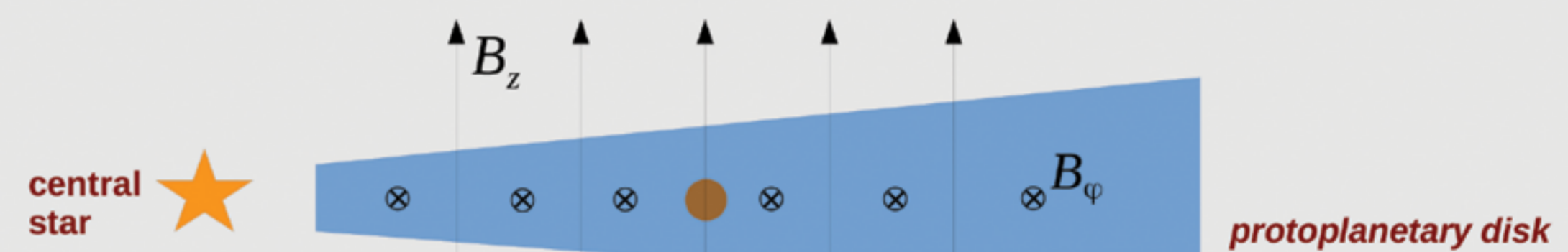
-Disks with vertical magnetic fields behave very differently from previously explored disks with pure (2D) azimuthal fields, in 2D and 3D vertical fields seem to *slow* planet migration (but not reverse it).
-A field with B_z and dB_ϕ/dz (a simplified wind model) increases regions of wave propagation in 2D and leads to 3-4 times stronger inwards migration than a disk with no field. In 3D, the Alfvén and magnetic resonances in this configuration exert the same sign of torque on both sides of planet, leading to fast inwards migration and a lack of convergence for the torque with azimuthal mode m .

Numerical MHD simulations

The protoplanetary disk

The disk is modeled as a sub-Keplerian rotating fluid in two and three dimensions. The geometry is cylindrical (r, ϕ, z). The gas feels the radial component of the stellar gravity, and it is vertically unstratified. The disk is threaded by a strong and uniform magnetic field of the general form

$$\mathbf{B} = (0, B_\phi r^{-q_\phi}, B_z r^{-q_z})$$



The planet

The planet is assumed to move in a fixed, circular orbit, and is included in the simulation as an extra gravitational potential felt by the circumstellar disk. This potential has the form

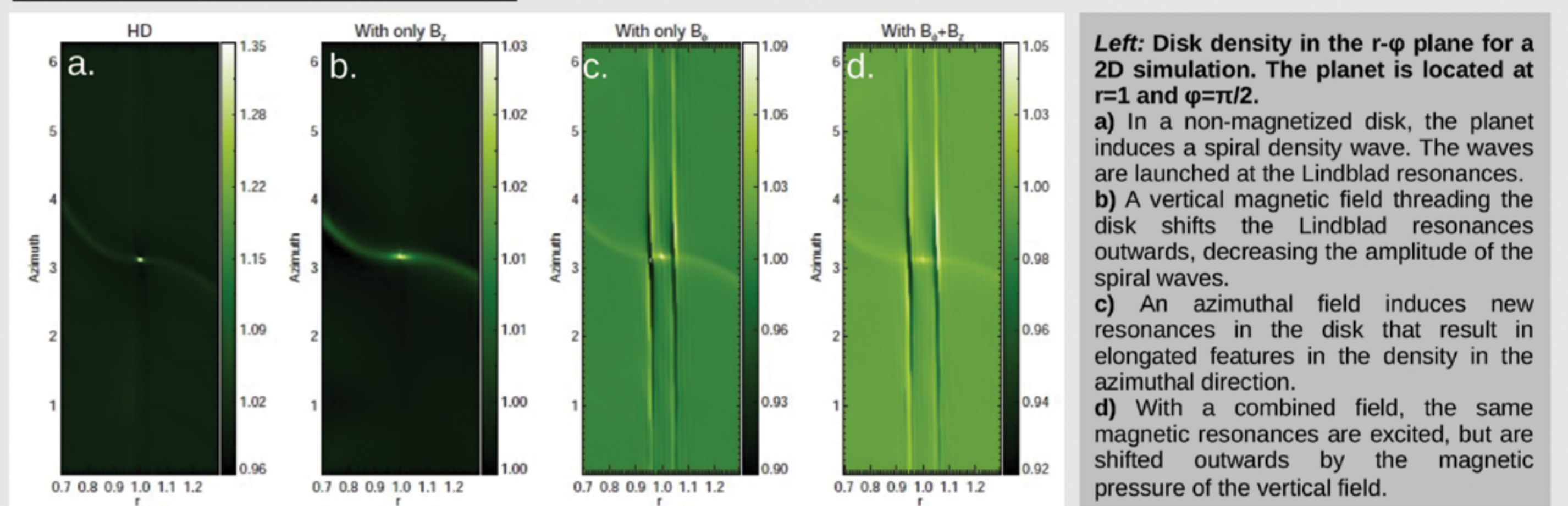
$$\Psi(r) = \frac{GM_p}{(|r-r_p|^2 + \epsilon^2)^{1/2}}$$

M_p planet mass
 G gravitational constant
 ϵ numerical softening

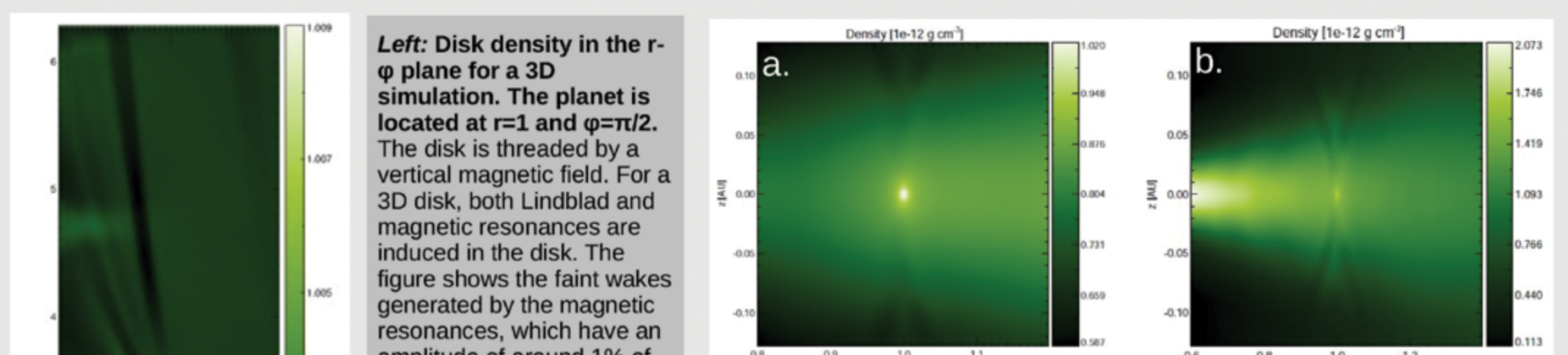
Code and Setup

Our numerical simulations are performed with version 4.0 of the PLUTO code (Mignone et al. 2007). We employ the HLLC and HLLD approximate Riemann solvers for, respectively, HD and MHD computations, and use a second-order piecewise parabolic spatial interpolation method and a second-order Runge-Kutta solver for time integrations. The Constrained Transport method is adopted in the MHD simulations to preserve a divergence-free magnetic field. Our calculations are carried out in the ideal regime (no explicit viscosity or resistivity) in either polar (2D) or cylindrical (3D) coordinates (see Uribe, Bans & König (2014)).

Planet-disk interaction



Left: Disk density in the $r-\phi$ plane for a 2D simulation. The planet is located at $r=1$ and $\phi=\pi/2$.
a) In a non-magnetized disk, the planet induces a spiral density wave. The waves are launched at the Lindblad resonances.
b) A vertical magnetic field threading the disk shifts the Lindblad resonances outwards, decreasing the amplitude of the spiral waves.
c) An azimuthal field induces new resonances in the disk that result in elongated features in the density in the azimuthal direction.
d) With a combined field, the same magnetic resonances are excited, but are shifted outwards by the magnetic pressure of the vertical field.



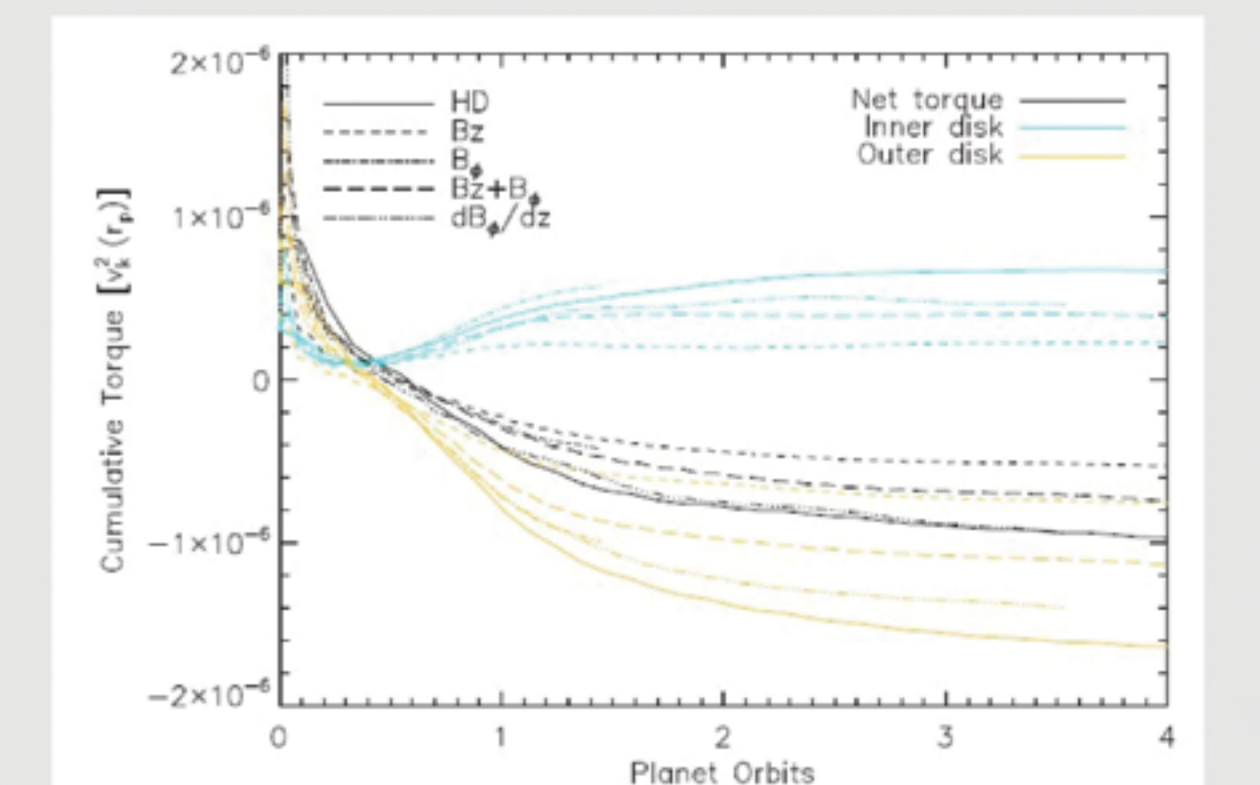
Left: Disk density in the $r-\phi$ plane for a 3D simulation. The planet is located at $r=1$ and $\phi=\pi/2$. The disk is threaded by a vertical magnetic field. For a 3D disk, both Lindblad and magnetic resonances are induced in the disk. The figure shows the faint wakes generated by the magnetic resonances, which have an amplitude of around 1% of the unperturbed density. Multiple spiral waves are generated due to the dependence of the position of the resonance with the azimuthal wave number of the perturbation, so that different modes are excited at different radial locations away from the planet. The density perturbations contribute to the total torque on the planet, which can lead to orbital migration. The closer the structure is to the planet, the larger is the coupling with the gravity of the planet.
Top: Disk density in the $r-z$ plane for a 3D simulation. The planet is located at $r=1$ and $z=0$. The snapshot shows a cut through the disk at the azimuthal location of the planet.
a) The disk is threaded by an azimuthal field of the form $B_\phi = B_\phi z$. The field is zero in the mid-plane and grows with z . This field geometry more closely mimics the large-scale field configuration of wind-driving disks. The variation of the field with z creates a vertical force that points towards the mid-plane and "squeezes" the disk, i.e. the pressure scale height decreases. Two "V"-shaped perturbations can be seen around the planet, which result from the magnetic resonances. In three dimensions, the plasma beta decreases with height, which results in the shift outwards with height of the location of the magnetic resonances.
b) When the stellar vertical gravity of the star, in addition to the vertical magnetic Lorentz force induced by the azimuthal field.

Radial migration

The rate of migration of the planet (a/\dot{a}) is estimated by calculating the gravitational specific torque exerted by the disk on the planet:

$$\Gamma_r = G \int \rho(r) \frac{(r_p \times r)}{|r-r_p|^3} dz \quad \text{and} \quad \Gamma_r \propto \dot{a}/a$$

The figure on the right shows the cumulative torque for different field configurations for the 3D simulations. A vertical field decreases the torque on the planet (short dashed line) with respect to the non-magnetized case (solid line) by about a factor of 2. A combined field with vertical and azimuthal components of the magnetic field (long dashed line) increases the torque with respect to the pure vertical field case, due to the additional magnetic resonances that appear in the mid-plane. A purely azimuthal field (dash-dotted line) will lead to instabilities that lead to turbulence. When the azimuthal field closely resembles the geometry of wind-driving disks, the torque is similar to that on a non-magnetized disk, due to the fact that the magnetic resonances only appear above the mid-plane.



Acknowledgments

Simulations were performed on the Midway supercomputer of the Research Computing Center of the University of Chicago.

References

- Bans, A., König, A., Uribe, A., Astrophysical Journal (2014) submitted.
- Uribe, A., Bans, A., König, A., Astrophysical Journal (2014) submitted.
- Mignone, A., Bodo, G., Massaglia, S., et al. (2007), ApJS, 170